Biochem. J. (2015) **465**, 175–184 (Printed in Great Britain) doi:10.1042/BJ20140833

Synthetic DAF-12 modulators with potential use in controlling the nematode life cycle

María V. Dansey*, Lautaro D. Alvarez†, Gisela Samaja†, Daiana S. Escudero‡, Adriana S. Veleiro†, Adalí Pecci*, Olga A. Castro‡[1] and Gerardo Burton†[1]

*Departamento de Química Biológica and IFIBYNE (CONICET-UBA), Facultad de Ciencias Exactas y Naturales, Universidad de Buenos Aires, Pabellón 2, Ciudad Universitaria, C1428EGA Buenos Aires, Argentina

†Departamento de Química Orgánica and UMYMFOR (CONICET-UBA), Facultad de Ciencias Exactas y Naturales, Universidad de Buenos Aires, Pabellón 2, Ciudad Universitaria, C1428EGA Buenos Aires, Argentina

‡Departamento de Química Biológica and IQUIBICEN (CONICET-UBA), Facultad de Ciencias Exactas y Naturales, Universidad de Buenos Aires, Pabellón 2, Ciudad Universitaria, C1428EGA Buenos Aires, Argentina

Dafachronic acids (DAs) are 3-keto cholestenoic acids bearing a carboxylic acid moiety at the end of the steroid side chain. These compounds interact with the DAF-12 receptor, a ligand-dependent transcription factor that acts as a molecular switch mediating the choice between arrest at diapause or progression to reproductive development and adult lifespan in different nematodes. Recently, we reported that the 27-nor-Δ^4-DA was able to directly activate DAF-12 in a transactivation cell-based luciferase assay and rescued the Mig phenotype of *daf-9*(*rh50*) *Caenorhabditis elegans* mutants. In the present paper, to investigate further the relationship between the structure of the steroid side chain and DAF-12 activity, we evaluated the *in vitro* and *in vivo* activity of Δ^4-DA analogues with modified side chains using transactivation cell-based assays and *daf-9*(*dh6*) *C. elegans* mutants. Our results revealed that introduction of a 24,25-double bond on the cholestenoic acid side chain did not affect DAF-12 activity, whereas shortening the side chain lowered the activity. Most interestingly, the C_{24} alcohol 24-hydroxy-4-cholen-3-one (**6**) was an antagonist of the DAF-12 receptor both *in vitro* and *in vivo*.

Key words: *Caenorhabditis elegans*, *daf-9* mutant, DAF-12 receptor, dafachronic acid, molecular dynamics.

INTRODUCTION

Many biological processes, such as the mechanisms that govern developmental transitions, pathways that regulate lifespan and those involved in a number of diseases, are conserved between human and invertebrates. *Caenorhabditis elegans* is a model organism that has the potential to bridge the gap between *in vitro* and *in vivo* approaches in vertebrates to study the interaction between molecules and to test the therapeutic value of candidate compounds in drug discovery development. Results are, in many cases, predictive for drug–target interactions [1–3].

C. elegans has the ability to sense environmental quality and nutrient availability and adjusts rates of maturation accordingly. In favourable environments, i.e. plentiful food, moderate temperature and low population density, *C. elegans* develops from the embryo through four larval stages (L1–L4) separated by moults, into a sexually reproductive adult in approximately 3.5 days. After this so-called reproductive development, they produce progeny for a week and then typically live for another 2 weeks. In unfavourable environments, i.e. high population density, limiting food or high temperature, animals arrest development at an alternative third larval stage called the dauer diapause, which is specialized for survival and dispersal [4,5]. Dauer larvae are arrested before sexual maturity at a quiescent state, and are morphologically and metabolically distinct, highly stress-resistant and long-lived. Upon returning to favourable conditions, the dauer larva emerges from diapause, resumes feeding and continues to develop into a reproductive adult with a normal lifespan [6]. Environmental and physiological cues detected by multiple sensory neurons in the head are transduced through various signal transduction pathways [7]. Components of neurosensory structure and guanylate cyclase signalling are involved in sensing temperature, nutrients and dauer pheromone, which regulate secretion of insulin/IGF (insulin-like growth factor) and TGFβ (transforming growth factor β) peptides. In favourable environments, TGFβ and insulin/IGF hormones are produced activating their respective signal transduction pathways that converge within steroidogenic tissues [8] to promote production of the cholesterol-derived DAF-12 ligands called DAs (dafachronic acids) [9,10]. DAF-12 is a nuclear receptor which works as a molecular switch that mediates the choice between arrest at diapause or progression to reproductive development and also regulates adult lifespan [1,11,12]. DAF-12 ligand binding results in dissociation of the co-repressor DIN-1 to allow expression of DAF-12 target genes, such as the *let-7* family of miRNAs, and *lin-46*, *lin-28* and *lin-41*, that are necessary to promote L3 and adult programmes [13], whereas unliganded DAF-12 together with the co-repressor DIN-1S directs the dauer fate [14]. Additionally, ligand-dependent activation of the DAF-12 target genes *miR-84* and *miR-241*, two miRNAs of the conserved *let-7* family, is required for lifespan regulation in response to signals from reproductive tissues [11].

Abbreviations: DA, dafachronic acid; DMEM, Dulbecco's modified Eagle's medium; DMF, dimethylformamide; HEK, human embryonic kidney; HRMS, high-resolution MS; IGF, insulin-like growth factor; LXR, liver X receptor; NGM, nematode growth medium; TGFβ, transforming growth factor β; THF, tetrahydrofuran.

[1] Correspondence may be addressed to either of these authors (email ocastro@qb.fcen.uba.ar or burton@qo.fcen.uba.ar).

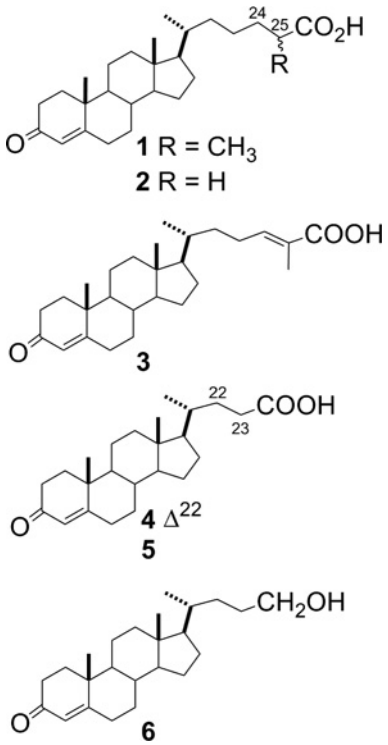

Figure 1 Structure of Δ^4-DAs (1) and the synthetic analogues 2–6

DAs are 3-keto cholestenoic acids in which one of the methyl groups at the end of the cholesterol side chain is oxidized to a carboxylic acid moiety [9,10]. This oxidation is the last step of DA biosynthesis and is carried out by DAF-9/CYP27A1, with chemistry orthologous to the mammalian CYP27A1 that is involved in bile acid biosynthetic pathways [9,15]. *C. elegans daf-9* mutants fall into two distinct classes. Strong loss-of-function mutants form dauer larvae constitutively (Daf-c) and weak loss-of-function mutants have penetrant heterochronic delays in L3 gonadal leader cell migrations (Mig), reduced fecundity and are slightly short-lived [16,17]. It is known that a C-3 keto group, an unsaturated double bond at C-4 (Δ^4) or C-7 (Δ^7), and an acidic carboxy group at the end of the cholesterol side chain are required for the efficient *Ce*DAF-12 activation (e.g. Δ^4-DA **1**, Figure 1). Moreover, the configuration of the C-25 methyl group would affect either ligand binding or complex conformation, since 25*S* diastereomers of both Δ^4 and Δ^7 DAs were shown to be more active than the corresponding 25*R* isomers [18]. It has been reported previously that Δ^4- and Δ^7-DA are the endogenous DAF-12 ligands [9], but recently Mahanti et al. [10] identified new DAF-12 ligands and their results indicate that $\Delta^{1,7}$-DA and Δ^7-DA are high-affinity ligands of DAF-12, whereas they did not find Δ^4-DA in their metabolomics analysis and concluded that Δ^4-DA may not be present at physiologically relevant concentrations, although its transient or very-low-level production cannot be excluded.

Recently, using a combination of molecular modelling, synthetic chemistry and biological experiments, we predicted and confirmed that the removal of the C-25 methyl in Δ^4-DAs does not abolish the *in vitro* or *in vivo* activity. We prepared the 27-nor-Δ^4-DA **2** (Figure 1) and evaluated its activity *in vivo*, where it rescued the Mig phenotype of *daf-9*(*rh50*) *C. elegans* mutants. This compound was also able to activate DAF-12 directly in a transactivation cell-based luciferase reporter assay, although it was less active than the corresponding 25*R*- and 25*S*-DAs [19,20]. To investigate further the relationship between the structure of the steroid side chain and the DAF-12 activity, we have now evaluated the biological activity *in vitro* and *in vivo* of the cholestenoic acid **3**, the cholenic acids **4** and **5** and the C_{24} alcohol **6** (Figure 1). The results revealed that DAF-12 activity may be modulated by structural modification of the steroid side chain. Thus we found that compound **3** acts as a pure agonist while alcohol **6** exhibited exceptional antagonist properties both in *in vitro* and *in vivo* assays.

EXPERIMENTAL

Chemistry

Melting points were taken on a Fisher–Johns apparatus and are uncorrected. NMR spectra were recorded on Bruker ACE-200 (^{1}H at 200.13 MHz, ^{13}C at 50.32 MHz) or Avance II 500 (^{1}H at 500.13 MHz, ^{13}C at 125.77 MHz) spectrometers. Chemical shifts are given in p.p.m. downfield from TMS (tetramethylsilane) as internal standard, *J* values are given in Hz. Multiplicity determinations and 2D spectra (COSY, NOESY, HSQC and HMBC) were obtained using standard Bruker software. Exact mass spectra [HRMS (high-resolution MS)] were obtained using a Bruker micrOTOF-Q II mass spectrometer, equipped with an ESI source operating in positive mode. Flash column chromatography was carried out on silica gel (0.040–0.063 mm). TLC analysis was performed on silica gel 60 F254 (0.2 mm thick). The homogeneity of all compounds was confirmed by TLC. Solvents were evaporated at reduced pressure and ~40–50 °C. Methyl 3β-hydroxy-5-cholenate (**7**) was prepared from 3α,6α-dihydroxy-5β-cholanic acid (Sigma), essentially following the procedure of Gioiello et al. [21]. Compounds **4**–**6** were obtained from 20β-carboxyaldehyde-4-pregnen-3-one (see the Supplementary Online Data).

3β-(t-Butyldimethylsilyloxy)-5-cholenic acid methyl ester (**8**)

Imidazole (126 mg, 1.85 mmol) and t-butyldimethylsilyl chloride (186 mg, 1.24 mmol) were added successively to a solution methyl ester **7** (123 mg, 0.317 mmol) in anhydrous DMF (dimethylformamide) (3 ml) and the solution was stirred for 1 h at room temperature under a nitrogen atmosphere. The reaction mixture was extracted with ether and the organic layer was washed successively with brine and water and dried with sodium sulfate. Evaporation of the solvent followed by flash chromatography (hexane/ethyl acetate, 97:3) gave the 3-silyl ether **8** (143 mg, 90 %). δ_H [500 MHz, (^{2}H)chloroform] 5.31 (1 H, dt, *J* 5 and 2 Hz, H-6], 3.66 (3 H, s, OCH_3], 3.48 (1 H, m, H-3], 2.35 (1 H, ddd, *J* 16, 10 and 5 Hz, H-23a), 2.26 (1 H, td, *J* 13 and 2 Hz, H-4β), 2.22 (1 H, m, H-23b), 2.16 (1 H, m, H-4α), 2.00 (1 H, dt, *J* 13 and 3 Hz, H-12β), 1.97 (1 H, m, H-7β), 1.86 (1 H, m, H-16α), 1.81 (1 H, dt, *J* 14 and 3 Hz, H-1β), 1.79 (1 H, m, H-22a), 1.71 (1 H, m, H-2α), 1.60 (1 H, m, H-15α), 1.53 (1 H, m, H-2β), 1.52 (1 H, m, H-7α), 1.49 (2 H, m, H-11), 1.46 (1 H, m, H-8), 1.42 (1 H, m, H-20), 1.33 (1 H, m, H-22b), 1.30 (1 H, m, H-16β), 1.15 (1 H, td, *J* 13 and 4 Hz, H-12α), 1.08 (1 H, m, H-15β), 1.03 (1 H, m, H-1α), 1.01 (1 H, m, H-17), 1.00 (3 H, s, H-19), 0.99 (1 H, m, H-14), 0.92 (3 H, d, *J* 7 Hz, H-21), 0.92 (1 H, m, H-9), 0.89 [9H, s, (CH_3)$_3$C-Si], 0.67 (3 H, s, H-18), 0.06 [6H, s, (CH_3)$_2$-Si]. δ_C [125 MHz, (^{2}H)chloroform] 174.8 (C-24), 141.5 (C-5), 121.1 (C-6), 72.6 (C-3), 56.8 (C-14), 55.7 (C-17), 50.2 (C-9), 42.8 (C-4), 42.4 (C-13), 39.8 (C-12), 37.4 (C-1), 36.4 (C-10), 35.4 (C-20), 31.9 (C-2), 31.9 (C-7 and C-8), 31.04 (C-23), 31.00 (C-22), 28.1 (C-16), 25.9 [(CH_3)$_3$C-Si], 24.2 (C-15), 21.0 (C-11), 19.4 (C-19), 18.29 (C-21), 18.26 [(CH_3)$_3C$-Si], 11.8 (C-18),

− 4.6 [(CH_3)$_2$-Si]; ESI–HRMS *m/z*: calculated for $C_{31}H_{54}NaO_3Si$ $[M+H]^+$ 525.3734, found 525.3723.

3β-(t-Butyldimethylsilyloxy)-5,24-cholestadien-27-oic acid ethyl ester (**11**)

The 3-silyl ether **8** obtained above (141 mg, 0.281 mmol) was stirred with lithium aluminium hydride (26.3 mg, 0.696 mmol) in dry tetrahydrofuran (7.0 ml) for 30 min under a nitrogen atmosphere. Ethyl acetate and a saturated aqueous solution of potassium sodium tartrate were added. The mixture was extracted with ethyl acetate and the organic layer was washed with water and dried with sodium sulfate. Evaporation of the solvent followed by flash chromatography (hexane/ethyl acetate, 100:0→90:10) gave compound **9** (116 mg, 87 %). δ_H [500 MHz, (^{2}H)chloroform] 5.32 (1 H, m, H-6), 3.62 (2 H, m, H-24), 3.48 (1 H, m, H-3), 2.26 (1 H, m, H-4β), 2.17 (1 H, ddd, *J* 13, 5 and 2 Hz, H-4α), 2.00 (1 H, m, H-12β), 1.98 (1 H, m, H-7β), 1.97 (1 H, m, H-22a), 1.84 (1 H, m, H-16α), 1.81 (1 H, dt, *J* 13 and 4 Hz, H-1β), 1.72 (1 H, m, H-2α), 1.65 (1 H, m, H-23a), 1.59 (1 H, m, H-15α), 1.54 (1 H, m, H-2β), 1.53 (1 H, m, H-7α), 1.47 (2 H, m, H-11), 1.45 (1 H, m, H-23b), 1.44 (1 H, m, H-8), 1.42 (1 H, m, H-20), 1.27 (1 H, m, H-16β), 1.16 (1 H, m, H-12α), 1.12 (1 H, m, H-17), 1.08 (1 H, m, H-15β), 1.07 (1 H, m, H-22b), 1.04 (1 H, m, H-1α), 1.00 (3 H, s, H-19), 0.99 (1 H, m, H-14), 0.94 (3 H, d, *J* 7 Hz, H-21), 0.92 (1 H, m, H-9), 0.89 [9 H, s, (CH_3)$_3$C-Si], 0.68 (3 H, s, H-18), 0.06 [6 H, s, (CH_3)$_2$-Si]. δ_C [125 MHz, (^{2}H)chloroform] 141.6 (C-5), 121.1 (C-6), 72.6 (C-3), 63.5 (C-24), 56.8 (C-14), 56.0 (C-17), 50.2 (C-9), 42.8 (C-4), 42.3 (C-13), 39.8 (C-12), 37.4 (C-1), 36.6 (C-10), 35.6 (C-20), 32.1 (C-2), 31.92 (C-7), 31.90 (C-8), 31.8 (C-22), 29.4 (C-23), 28.2 (C-16), 25.9 [(CH_3)$_3$C-Si], 24.3 (C-15), 21.1 (C-11), 19.4 (C-19), 18.7 (C-21), 18.2 [(CH_3)$_3$*C*-Si], 11.9 (C-18), − 4.6 [(CH_3)$_2$-Si]; ESI−HRMS *m/z*: calculated for $C_{30}H_{54}NaO_2Si$ $[M+H]^+$ 497.3785, found 497.3774.

A suspension of pyridinium chlorochromate (218 mg, 1.01 mmol), barium carbonate (64.7 mg, 0.34 mmol) and 3 Å (1 Å = 0.1 nm) molecular sieves (221 mg) in anhydrous dichloromethane (5 ml) was stirred for 5 min under a nitrogen atmosphere at room temperature. A solution of **9** (114 mg, 0.240 mmol) in anhydrous dichloromethane (5 ml) was added and stirring continued at room temperature for 40 min. The reaction mixture was diluted with ether and percolated through silica gel with ethyl acetate. Evaporation of the solvent gave compound **10** (93.0 mg, 82 %). δ_H [500 MHz, (^{2}H)chloroform] 9.77 (1 H, s, H-24), 5.32 (1 H, dt, *J* 5 and 2 Hz, H-6), 3.48 (1 H, m, H-3), 2.45 (1 H, ddd, *J* 15, 6 and 2 Hz, H-23a), 2.36 (1 H, m, H-23b), 2.26 (1 H, m, H-4β), 2.18 (1 H, m, H-4α), 2.00 (1 H, m, H-12β), 1.98 (1 H, m, H-7β), 1.85 (1 H, m, H-16α), 1.81 (1 H, m, H-1β), 1.80 (1 H, m, H-22b), 1.72 (1 H, m, H-2α), 1.61 (1 H, m, H-15α), 1.54 (1 H, m, H-2β), 1.52 (1 H, m, H-7α), 1.49 (2 H, m, H-11), 1.45 (2 H, m, H-8 and H-20), 1.33 (1 H, m, H-22a), 1.31 (1 H, m, H-16β), 1.16 (1 H, m, H-12α), 1.11 (1 H, m, H-17), 1.09 (1 H, m, H-15β), 1.04 (1 H, m, H-1α), 1.00 (3 H, s, H-19), 1.00 (1 H, m, H-14), 0.93 (3 H, d, *J* 7 Hz, H-21), 0.92 (1 H, m, H-9), 0.89 [9 H, s, (CH_3)$_3$C-Si], 0.68 (3 H, s, H-18), 0.06 [6 H, s, (CH_3)$_2$-Si]. δ_C [125 MHz, (^{2}H)chloroform] 203.2 (C-24), 141.6 (C-5), 121.1(C-6), 72.6 (C-3), 56.8 (C-14), 55.8 (C-17), 50.2 (C-9), 42.8 (C-4), 42.4 (C-13), 40.9 (C-23), 39.8 (C-12), 37.4 (C-1), 36.3 (C-10), 35.3 (C-20), 32.1 (C-2), 31.9 (C-7 and C-8), 28.2 (C-16), 28.0 (C-22), 25.9 [(CH_3)$_3$C-Si], 24.3 (C-15), 21.0 (C-11), 19.4 (C-19), 18.4 (C-21), 18.2 [(CH_3)$_3$*C*-Si], 11.9 (C-18), − 4.6 [(CH_3)$_2$-Si]; ESI–HRMS *m/z*: calculated for $C_{30}H_{52}NaO_2Si$ $[M+H]^+$ 495.3629, found 495.3624.

To a solution of **10** (92 mg, 0.195 mmol) in dichloromethane (3 ml) was added (1-carbethoxyethyl)-triphenylphosphonium bromide (106 mg, 0.238 mmol). A saturated aqueous solution of sodium bicarbonate (2.0 ml) was heated at 100 °C and poured over the suspension. The reaction mixture was stirred at 50 °C for 1 h, allowed to cool at room temperature and extracted with dichloromethane. The organic layer was dried with sodium sulfate and the solvent evaporated under vacuum. The resulting solid was purified by flash chromatography (hexane/ethyl acetate, 97:3→90:10) to give **11** (65 mg, 60 %). δ_H [500 MHz, (^{2}H)chloroform] 6.74 (1 H, td, *J* 8 and 2 Hz, H-24), 5.32 (1 H, m H-6), 4.18 (2 H, q, *J* 7 Hz, OCH_2CH$_3$), 3.48 (1 H, m, H-3), 2.27 (1 H, m, H-4α), 2.21 (1 H, m, H-23a), 2.07 (1 H, m, H-23b), 2.19 (1 H, m, H-4β), 2.01 (1 H, m, H-12β), 1.97 (1 H, m, H-7β), 1.84 (1 H, m, H-16α), 1.83 (1 H, m, H-27), 1.82 (1 H, m, H-1β), 1.72 (1 H, m, H-2α), 1.59 (1 H, m, H-15α), 1.54 (1 H, m, H-2β), 1.53 (2 H, m, H-22b and H-7α), 1.48 (2 H, m, H-11), 1.45 (2 H, m, H-8 and H-9), 1.43 (1 H, m, H-20), 1.29 (3 H, t, *J* 7 Hz, OCH$_2$CH_3), 1.27 (1 H, m, H-16β), 1.17 (1 H, m, H-22a), 1.17 (1 H, m, H-12α), 1.12 (1 H, m, H-17), 1.05 (1 H, m, H-1α), 1.03 (1 H, m, H-15β), 1.00 (3 H, s, H-19), 0.99 (1 H, m, H-14), 0.95 (3 H, d, *J* 7 Hz, H-21), 0.89 [9H, s, (CH_3)$_3$C-Si], 0.68 (3 H, s, H-18), 0.06 [6H, s, (CH_3)$_2$-Si]. δ_C [125 MHz, (^{2}H)chloroform] 166.8 (C-26), 150.0 (C-24), 121.0 (C-25), 141.6 (C-5), 121.1 (C-6), 72.6 (C-3), 60.4 (OCH_2CH$_3$), 56.8 (C-14), 55.9 (C-17), 50.2 (C-9), 42.8 (C-4), 42.4 (C-13), 39.8 (C-12), 37.4 (C-1), 36.6 (C-10), 35.7 (C-20), 32.1 (C-2), 31.9 (C-7), 31.9 (C-8), 25.4 (C-23), 34.7 (C-22), 28.2 (C-16), 25.9 [(CH_3)$_3$C-Si], 24.3 (C-15), 21.1 (C-11), 19.4 (C-19), 18.6 [(CH_3)$_3$*C*-Si],18.5 (C-21), 14.3 (OCH$_2$*C*H$_3$), 12.28 (C-27), 11.9 (C-18), − 4.6 [(CH_3)$_2$-Si]; ESI–HRMS *m/z*: calculated for $C_{35}H_{60}NaO_3Si$ $[M+H]^+$ 579.4204, found 579.4195.

3-Oxo-4,24-cholestadien-27-oic acid (**3**)

To a solution of **11** (63 mg, 0.113 mmol) in THF (tetrahydrofuran) (5 ml) and acetonitrile (5 ml), was added 40 % hydrofluoric acid (1.4 ml) and the solution was stirred for 1 h at 0 °C. The reaction mixture was neutralized with aqueous potassium carbonate and extracted with ethyl acetate. The organic layer was washed with water, dried with sodium sulfate and the solvent was evaporated under vacuum to give compound **12** (45.0 mg, 90 %); δ_H [200 MHz, (^{2}H)chloroform] 6.76 (1 H, t, *J* 8 Hz, H-24), 5.32 (1 H, broad s, H-6), 4.20 (2 H, q, *J* 7 Hz, OCH_2CH$_3$), 3.52 (1 H, m, H-3), 1.83 (3 H, s, H-27), 1.30 (3 H, t, *J* 7 Hz, OCH$_2$CH_3), 1.01 (3 H, s, H-19), 0.96 (3 H, d, *J* 7 Hz, H-21), 0.69 (3 H, s, H-18).

Compound **12** (43.0 mg, 0.0972 mmol) was treated following the same procedure described for compound **10** to give the corresponding 3-ketosteroid (35.0 mg, 81 %); δ_H [200 MHz, (^{2}H)chloroform] 6.75 (1 H, t, *J* 8 Hz, H-24), 5.36 (1 H, broad s, H-6), 4.20 (2 H, q, *J* 7 Hz, OCH_2CH$_3$), 3.52 (1 H, m, H-3), 3.30 (1 H, d, *J* 18 Hz, H-4a), 2.82 (1 H, d, *J* 18 Hz, H-4b),1.84 (3 H, s, H-27), 1.30 (3 H, t, *J* 7 Hz, OCH$_2$CH_3), 1.26 (3 H, s, H-19), 0.97 (3 H, d, *J* 7 Hz, H-21), 0.72 (3 H, s, H-18). To a solution of the 3-ketosteroid obtained above (32.0 mg, 0.0726 mmol) in methanol (3 ml), 20 % aqueous potassium carbonate solution was added (1.5 ml). The reaction mixture was stirred at 50 °C for 3 h, allowed to cool to room temperature and acidified (pH 3) with 1 M HCl. After extraction with ethyl acetate, the organic layer was washed with water, dried with sodium sulfate and the solvent evaporated under vacuum. The resulting solid was purified by flash chromatography (ethyl acetate/hexane, 95:5→80.20) to give acid **3** (15 mg, 50 %) as a white solid, melting point 208–209 °C. δ_H [500 MHz, (^{2}H)chloroform] 6.89 (1 H, ddd, *J* 1, 8 and 15 Hz, H-24), 5.73 (1 H, s, H-4), 2.42 (1 H, m, H-2β), 2.38 (1 H, m, H-6β), 2.34 (1 H, m, H-2α), 2.22 (1 H, m, H-23a), 2.11 (1 H, m, H-23b), 2.03 (1 H, m, H-12β), 2.02 (1 H, m, H-1β), 1.86

(1 H, m, H-16α), 1.84 (1 H, m, H-7β), 1.84 (1 H, s, H-27), 1.69 (1 H, m, H-1α), 1.54 (1 H, m, H-22b), 1.53 (1 H, m, H-11α), 1.52 (1 H, m, H-20), 1.44 (2 H, m, H-8 and H-11β), 1.29 (1 H, m, H-16β), 1.62 (1 H, m, H-15β), 1.18 (3 H, s, H-19), 1.17 (2 H, m, H-12α and H-22a), 1.13 (1 H, m, H-17), 1.12 (1 H, m, H-15α), 1.02 (2 H, m, H-14 and H-7α), 0.96 (3 H, d, J 7 Hz, H-21), 0.92 (1 H, m, H-9), 0.72 (3 H, s, H-18). δ_C [125 MHz, (^{2}H)chloroform] 199.7 (C-3), 172.9 (C-26), 171.7 (C-5), 145.6 (C-24), 126.7 (C-25), 55.9 (C-14), 55.8 (C-17), 53.8 (C-9), 123.7 (C-4), 42.5 (C-13), 39.6 (C-12), 38.6 (C-10), 35.7 (C-1), 35.59 (C-8), 35.58 (C-20), 34.5 (C-22), 33.9 (C-2), 32.9 (C-6), 32.0 (C-7), 28.2 (C-16), 25.6 (C-23), 24.1 (C-15), 21.0 (C-11), 18.4 (C-21), 17.4 (C-19), 11.9 (C-18 and C-27), ESI–HRMS *m/z*: calculated for $C_{27}H_{41}O_3$ $[M+H]^+$ 413.3050, found 413.3063.

Biological activity

Cell culture and reporter assays

HEK (human embryonic kidney)-293T cells were cultured in DMEM (Dulbecco's modified Eagle's medium) supplemented with 10% (v/v) FBS containing 100 IU/ml penicillin and 100 μg/ml streptomycin. Reporter assays were performed by transfecting HEK-293T cells with Lipofectamine® 2000 (Invitrogen) in 12-well plates with serum-free DMEM as described in [13]. Then on one hand, 400 ng of pCMV myc DAF-12 A1 vector were co-transfected with 6 ng of pGL3 Luc with *Let-70* promoter and 280 ng of CMX-β-galactosidase as transfection efficiency control. On the other, 250 ng of MH100×4-tk–luciferase, 200 ng of CMX-β-galactosidase as transfection efficiency control and 670 ng of CMX-Gal4-DAF-12LBD, which expresses a fusion protein of the Gal4 DNA-binding domain with the ligand-binding domain of the DAF-12 receptor (referred to as Gal4-DAF-12-LBD). At 6 h after transfections, ligands were added (applied from a stock solution in DMSO), and luciferase and β-galactosidase activities were measured 16–24 h after the addition of ligands or vehicle control. Each experiment was repeated three times and fold activation is relative to the non-stimulated control, unless indicated otherwise.

C. elegans strains and nematode culture

C. elegans was cultured at 20 °C unless indicated otherwise, on NGM (nematode growth medium) plates with *Escherichia coli* OP50 bacterial lawn. Wild-type N2 Bristol was provided by the *C. elegans* Genetics Center, University of Minnesota (Minneapolis, MN, U.S.A.) and *daf-9*(*dh6*) *dhEx24* by Dr Adam Antebi, Max Planck Institute for Biology of Ageing (Cologne, Germany).

Dauer larvae rescue assays

Appropriate amounts of compound **2** or **3** were diluted in ethanol and added to NGM to give the indicated concentrations; plates were dried and seeded with OP50 *E. coli*. *daf-9*(*dh6*) *dhEx24* gravid hermaphrodites were allowed to lay eggs in plates containing compound **2**, compound **3** or ethanol as control for 4 h and removed from plates. Plates containing a mixture of *daf-9*(+), *gfp*(+) and *daf-9*(−), *gfp*(−) embryos were incubated at 20 °C and *daf-9*(*dh6*) *gfp*(−) were transferred to a fresh plate and scored for dauer arrest 72 h after hatching. Final concentrations refer to the amount plated in agar (3–4 ml/plate).

Antagonist activity assays

Wild-type gravid hermaphrodites were allowed to lay eggs in plates containing 10 μM compound **6** alone, 10 μM compound **6** plus increasing concentrations of compound **3** or ethanol as control and then removed from plates. Plates were incubated at 18 °C and developmental stages were analysed every 24 h for 5 days. Additionally, nematodes developed in plates containing 10 μM compound **6** at 18 °C for 2 days were transferred to fresh plates devoid of compound **6** and developmental stages were scored every 24 h for another 3 days. Plates were prepared as indicated in larva dauer rescue assay.

Computational methods

MD were performed by using the Amber 12 software package (http://ambermd.org/). For the MD simulation, the starting receptor structure was taken from the previously developed *Ce*DAF-12/25*R*-Δ^7-DA model [19]. The *Ce*DAF-12–**3** and *Ce*DAF-12–**6** complexes were built *in silico*, superposing the B and C ring carbon atoms of HF/6-31G** optimized structures obtained using the quantum chemistry program Gaussian 03 (http://www.gaussian.com/), with the corresponding atoms of the 25*R*-Δ^7-DA molecule. The ligand parameters were assigned according to the GAFF (general Amber force field) and the corresponding RESP (restraint electrostatic potential) atomic partial charges at HF/6-31G** level. The Amber99 force field parameters were used for all receptor residues [22]. The complexes were immersed in an octahedral box of TIP3P (transferable intermolecular potential 3P) water molecules, giving final systems of approximately 26000 atoms. The systems were initially optimized and then gradually heated to a final temperature of 300 K. Starting from these equilibrated structures, MD production runs of 50 ns were obtained for each complex. All simulations were performed at 1 atm (1 atm = 101.325 kPa) and 300 K, maintained with the Berendsen barostat and thermostat respectively [23] using periodic boundary conditions and the particle mesh Ewald method (grid spacing of 1 Å) for treating long-range electrostatic interactions with a uniform neutralizing plasma. The SHAKE algorithm was used to keep bonds involving hydrogen atoms at their equilibrium length, allowing the use of a 2 fs time step for the integration of Newton's equations.

RESULTS

Chemistry

The synthetic analogues were selected so as to evaluate the influence on receptor activation of the length and flexibility of the ligand side chain. Thus compound **3**, with an additional double bound at C-24, has reduced side-chain flexibility compared with the natural ligands Δ^4-DA (**1**). On the other hand, taking into account that *in silico* simulations indicated that the side chain of compound **2** does not adopt a fully extended conformation, but a torsioned one, we synthesized three analogues with a shortened side chain. Compounds **4** and **5** maintain the terminal carboxy group, whereas this group was replaced by a hydroxy group in compound **6**, modifying in this way the capacity of this compound to form hydrogen bonds with receptor residues. Besides, compound **6** has been proposed as an agonist of the human receptor LXR (liver X receptor), the protein sequence of which is most similar to *Ce*DAF-12 [24].

Compound **3** was synthesized as outlined in Scheme 1. Methyl ester **7** was prepared from 3α,6α-dihydroxy-5β-cholanic acid (hyodeoxycholic acid) following essentially the procedure of

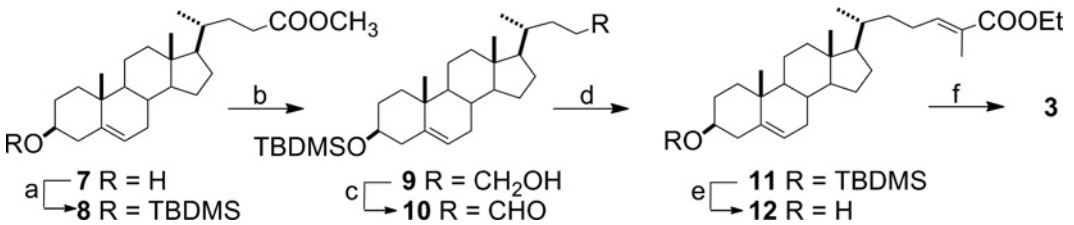

Scheme 1 Reagents and conditions

(a) t-Butyldimethylchlorosilane, imidazole, DMF, 25 °C (90 %); (b) lithium aluminium hydride, THF, 0 °C (87 %); (c) pyridinium chlorochromate, barium carbonate, molecular sieve (3 Å), dichloromethane (82 %); (d) (1-carbethoxyethyl)-triphenylphosphonium bromide, dichloromethane/sodium bicarbonate (aqueous), reflux (60 %); (e) hydrofluoric acid (40 %), THF/acetonitrile, 0 °C (90 %); (f) i. pyridinium chlorochromate, barium carbonate, molecular sieve (3 Å), dichloromethane (81 %); ii. potassium carbonate (aqueous), methanol, 50 °C (50 %).

Gioiello et al. [21] and the alcohol at C-3 was protected as silyl ether. The aldehyde **10** was obtained from **8** by reduction of the C-24 ester functionality using $LiAlH_4$, followed by oxidation with pyridinium chlorochromate (this procedure gave better overall yields than direct reduction with di-isobutylaluminum hydride). The 3-carbon homologation was carried out on the intermediate C-24 aldehyde using a Wittig reaction with (1-carbethoxyethylidene)-triphenylphosphorane generated *in situ*, to give **11.** The NOESY spectrum of this compound showed correlations between H-27 (δ 1.83) and hydrogen atoms at positions 23 (δ 2.07 and 2.21) indicating an *E* configuration of the $C_{24} = C_{25}$ double bond. Cleavage of the silyl ether with 40 % hydrofluoric acid gave **12**. Finally, oxidation of the alcohol at C-3 with pyridinium chlorochromate followed by basic hydrolysis (potassium carbonate in methanol/water) gave compound **3** (10 % yield from **7**). Preparation of the known compounds **4**, **5** and **6** is described in Supplementary Scheme S1.

Biological activity

Compounds **2** and **3** display agonist activity in reporter gene assays

The activity of compounds **2**–**6** was evaluated in HEK-293T cells co-transfected with an expression vector codifying the luciferase reporter gene under the control of *Gal4* promoter [9] and an expression vector expressing a chimaeric protein consisting of the DNA-binding domain of Gal4 fused to the DAF-12 ligand-binding domain. After transfections, concentration–response curves were created with the synthetic analogues (Figure 2A). Compound **3** behaved as a potent agonist, with an estimated EC_{50} of 0.8 ± 0.2 μM. Similar to compound **2** [20], compound **4** showed agonist activity only when it was administered at concentrations higher than 1 μM. Compounds **5** and **6** did not induce luciferase expression in the concentration range tested. Similar results were observed in HEK-293T cells co-transfected with the luciferase reporter vector controlled by the *atg-7*/*let-7* promoter of the region CEOP4404 operon containing the *atg-7* and *let-70* genes (strongly regulated by DAF-12) [13], together with the complete DAF-12 expression vector. Figure 2(B) shows that compound **3** had 4-fold increased luciferase activity when it was administered at 1 μM, whereas compounds **2** and **4** showed less activity even when they were administered at 10 μM. On the other hand, compounds **5** and **6** were unable to induce luciferase expression at the concentrations assayed.

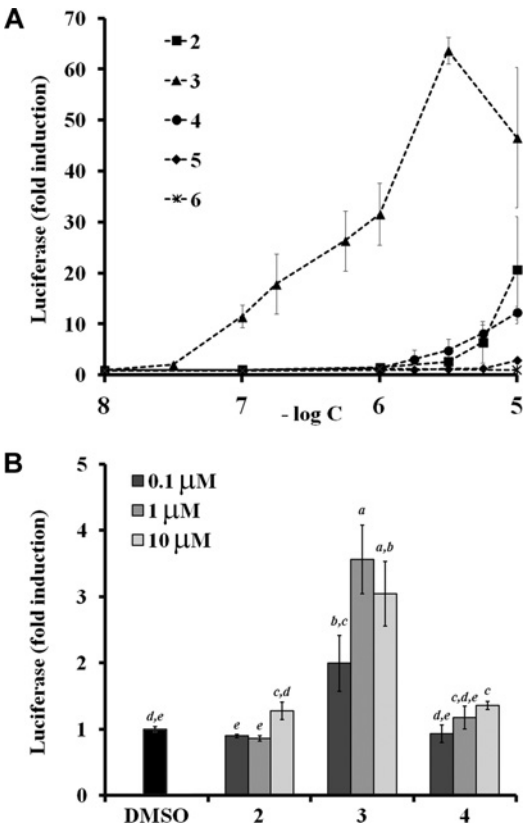

Figure 2 Activation of DAF-12 by compounds 2–6 in reporter gene assay

(**A**) Concentration-response of Gal4–DAF-12-dependent reporter activity in the presence of the compounds **2**–**6** in HEK-293T cells (means ± S.D.; $n = 3$); (**B**) DAF-12-dependent *atg-7*/*let-7*-luciferase reporter activity in the presence of increasing concentrations of compounds **2**–**6** in HEK-293T cells. Cytomegalovirus-LacZ vector (3 μg) was also introduced as control of transfection. Cells were incubated for 24 h with DMSO (control) or the different steroids. Luciferase activity was measured and corrected for β-galactosidase activity. Values are expressed as means ± S.E.M. fold induction relative to the controls. Statistical significance was determined using Tukey's test. In all cases, different letters indicate a significant difference between means ($P < 0.05$).

Compounds **2** and **3** rescue the Daf-c phenotype of *daf-9*-null allele

To characterize further compound **3**, we assayed its biological activity *in vivo* compared with 27-nor-Δ^4-DA **2**, using *daf-9*(*dh6*) nematodes defective in DA production. In the absence of exogenously added DAF-12 ligand, developing *daf-9*(*dh6*) nematodes arrest as dauer larvae because unliganded DAF-12 constitutively interacts with its co-repressor DIN-1 [14,25]. To score the ability of the exogenous added compounds to rescue the Daf-c phenotype, *daf-9*(*dh6*) nematodes were allowed to develop in NGM plates containing different amounts of compound **2**, compound **3** or ethanol alone as control. The development stage of nematodes was analysed at 24 h intervals for 6 days and the percentage of nematodes that had developed into young

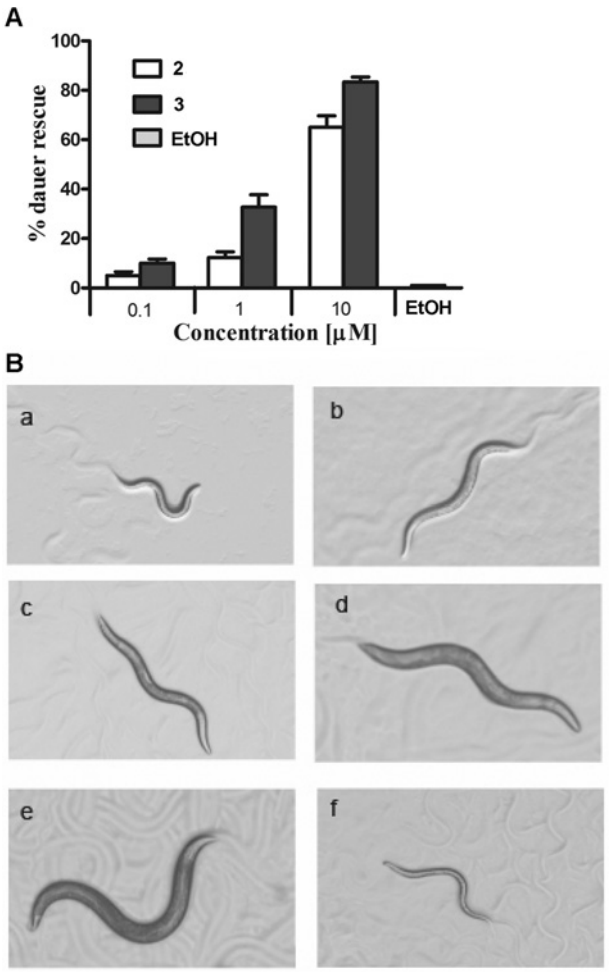

Figure 3 Compound 2 and 3 rescue the Daf-c phenotype of *daf-9*(*dh6*) mutant

C. elegans daf-9(*dh6*) and N2 wild-type nematodes were grown in the presence of the indicated concentrations of compound **2** (white bars), compound **3** (black bars) or ethanol (EtOH) (grey bar) at 20 °C. (**A**) Percentage of nematodes that developed into wild-type adults after 4 days. Results are means ± S.D. for three independent experiments with $n > 60$ nematodes. (**B**) Images of *daf-9*(*dh6*) nematodes (panels a–d and f) and wild-type nematodes (panel e) grown in plates containing 10 μM compound **2** (panels a and b), 10 μM compound **3** (panels c and d) or ethanol (panels e and f). Pictures were taken at day 3 (panels a, c and e) and day 6 (panels b, d and f) after hatching.

adults were determined at day 3 after hatching (Figure 3A). This assay scores the ability of the exogenously added compounds to rescue the Daf-c phenotype and to promote development to adulthood (providing a measure of the presence of a DAF-12 ligand that would dissociate the DAF-12–DIN-1 complex). We found that both compounds **2** and **3** were able to rescue the Daf-c phenotype in *daf-9*(*dh6*) nematodes in the range 0.1–10 μM. In the presence of 10 μM compound **2** or **3**, 65 % and 83 % of animals respectively bypassed dauer diapause to become reproductive adults. Compounds **2** and **3** also rescued larvae 12 % and 36 % respectively when applied at 1 μM (5 and 10 % respectively at 0.1 μM).

Wild-type nematodes developed in the presence of 10 μM compounds **2** or **3** or ethanol alone (Figure 3B, panel e), were young adults 48 h after hatching, showing that the exogenous addition of these compounds had no effect on wild-type growth rates. When *daf-9*(*dh6*) eggs were allowed to develop in the presence of ethanol alone, all of them produced

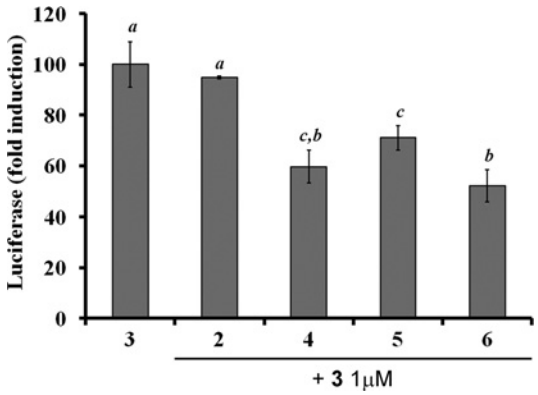

Figure 4 Antagonism of Gal4–DAF-12 activation by compounds 2 and 4–6

HEK-293T cells were co-transfected with pGal4-luciferase reporter and pGal4-DAF-12-LBD expression vector. Cells were then treated with 1 μM compound **3** in the absence or presence of 10 μM compound **2**, **4**, **5** or **6**. Luciferase fold induction is expressed relative to 1 μM compound **3** (100 %). Results are means ± S.E.M. ($n = 3$). Statistical significance was determined by Tukey's test. In all cases, different letters indicate a significant difference between means ($P < 0.05$).

dauer progeny, confirming the Daf-c phenotype of *daf-9*(*dh6*) nematodes (Figure 3B, panel f). To assess dauer recovery, we scored nematodes that displayed pharyngeal pumping [26]. In the presence of 10 μM compound **2** or **3**, *daf-9*(*dh6*) nematodes bypassed the dauer diapause 72 h after hatching and displayed a smaller size than wild-type nematodes, indicating a lower developmental rate. Moreover, nematodes developed in the presence of compound **2** were even smaller than those developed with compound **3** (Figure 3B, panels a and c). All rescued nematodes treated with compound **3** were young adults 72 h later (Figure 3B, panel d), turning into gravid hermaphrodites that laid eggs the day after. On the other hand, 30–40 % of the rescued nematodes developed in the presence of compound **2** showed a smaller size by the same time (Figure 3B, panel c) and needed 48 h more to develop into gravid hermaphrodites. Thus compound **3** behaved as a stronger DAF-12 ligand *in vivo* than compound **2** at all concentrations analysed (Figure 3A), but both compounds allowed the expression of DAF-12 target genes necessary to promote the L2/L3 switch and the larval to adult transition [13]. These results are consistent with those reported previously by our group [20] where we showed that 250 nM compound **2** was able to rescue the Mig phenotype of *daf-9*(*rh50*) mutant development, reversing the associated effects produced by the deficient biosynthesis of DA [16,27].

Compound **6** displays pure antagonist activity in reporter gene assays

Taking into account that analogue **3** was a pure agonist, antagonist effects of the other four compounds (**2** and **4**–**6**) were determined against compound **3**-dependent gene expression induction. HEK-293T cells were co-transfected with pGal4-luciferase reporter and pGal4-DAF-12LBD expression vector. Cells were then treated with 1 μM compound **3** in the absence or presence of compounds **2**, **4**, **5** and **6** at a concentration of 10 μM. Figure 4 shows that compounds **4**, **5** and **6** were able to inhibit the effect of compound **3**, with compounds **4** and **6** being the strongest inhibitors. Similar results were observed in HEK-293T cells co-transfected with the luciferase reporter vector controlled by the *atg-7*/*Let-7* promoter together with the complete DAF-12 expression vector. Compound **6** at 10 μM significantly decreased (~15 %, $P < 0.05$) the luciferase activity relative to agonist **3** at 1 μM, when they

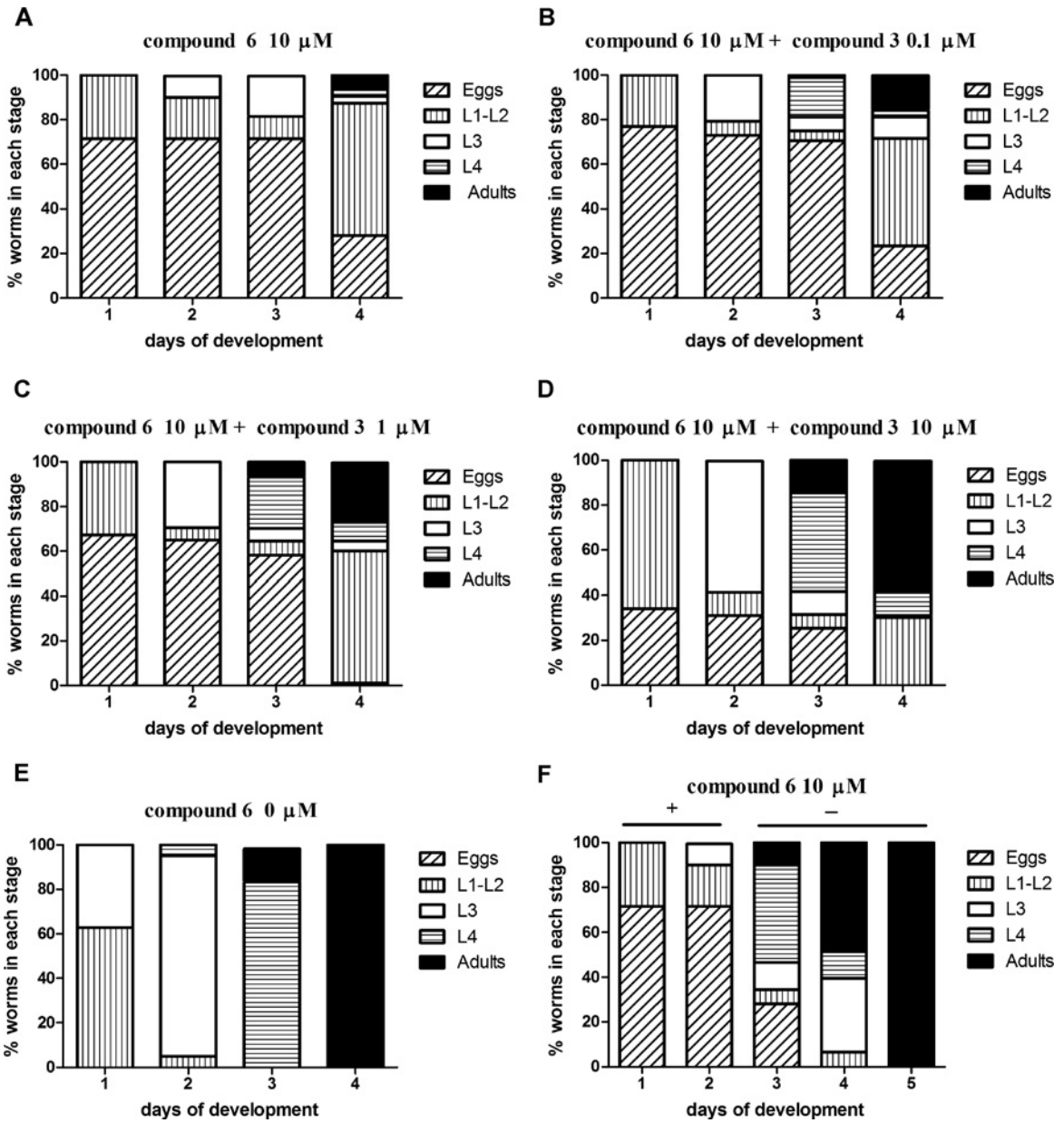

Figure 5 Compound 6 displays antagonist activity towards wild-type nematodes

N2 wild-type *C. elegans* were grown in the presence of 10 μM compound **6** (**A**), compound **6** in the presence of increasing doses of compound **3** (0.1, 1 and 10 μM; **B**, **C** and **D** respectively) or ethanol as control (**E**). Plates were incubated at 18°C. Developmental stages were analysed every 24 h for 5 days and the percentages of eggs, L1/L2, L3, L4 and adults were determined. N2 wild-type nematodes grown in the presence of 10 μM compound **6** for 2 days and then transferred to fresh plates in absence of compound **6** are shown in (**F**). Studies were performed for three independent cohorts ($n = 200$) and results are means for the three experiments.

were co-administered. According to these results, compound **6** arises as a putative DAF-12 pure antagonist and was chosen for further characterization.

Compound **6** displays antagonist activity *in vivo*

To analyse the antagonist effects of compound **6** *in vivo*, wild-type nematodes were allowed to develop in the presence or absence of a 10 μM concentration of this compound and the percentage of nematodes in each developmental stage was determined at 24 h intervals for 4 days (Figure 5A). This assay scores the ability of compound **6** to inhibit the effect of endogenous DAF-12 ligands. After 4 days, only 7 % of nematodes developed into adults and 28 % of the eggs remained unhatched in presence of compound **6**, with the remaining 65 % nematodes mostly developed into L1/L2, whereas 100 % of nematodes developed into adults in absence of this compound (Figure 5E). Some of the adults developed in the presence of compound **6** showed a smaller size than those developed in the absence of this compound. However, after 7 days, all nematodes developed into adults, suggesting the lack of toxicity of compound **6**. Furthermore, when wild-type eggs were developed in the presence of compound **6** for 2 days and then transferred to NGM fresh plates, almost 50 % of them developed into adults by day 4 and 100 % by day 5 (Figure 5F). This result demonstrates that, in the absence of compound **6**, the delay in development was overcome by the presence of endogenous

DAs and programmes that govern larval and adult development were restored. Taking into account that the analogue **3** behaved as a potent DAF-12 agonist *in vivo*, we analysed whether this compound was able to interfere with the antagonist effect of compound **6** *in vivo*. Wild-type nematodes were developed in the presence of 10 μM compound **6** and increasing concentrations of compound **3** (0.1, 1 and 10 μM) and the percentage of nematodes in each developmental stage was determined (Figures 5B, 5C and 5D respectively). Our results show that higher concentrations of compound **3** correspond to smaller delays in maturing to progressive larval stages. By day 4, we found both lower percentages of unhatched eggs (28 % and 23 % at 0 and 0.1 μM compound **3** respectively) and higher percentages of nematodes that reached adulthood (7, 16, 26 and 58 % at 0, 0.1, 1 and 10 μM compound **3** respectively). Moreover, no significant change in the development of nematodes was observed in the presence of 0.1, 1 and 10 μM compound **3** (Supplementary Figure S1). On this basis, we can conclude that both compounds are able to interact with the DAF-12 receptor, confirming the antagonist activity of compound **6**.

Ligand-binding mode of DA analogues

Taking into consideration the biological results depicted above, we were particularly interested in understanding at the molecular level how the receptor recognizes the structural differences in the side chain of the different steroids. In this sense, since compound **3**, a pure agonist, and compound **6**, a pure antagonist, correspond to opposite extremes of the DAF-12 activation state, we analysed their ligand-binding mode carrying out 50 ns MD simulations of the DAF-12–ligand complexes. The initial receptor structure was obtained from the co-ordinates of our *Ce*DAF-12/25*S*-Δ^7-DA model [19]. Compounds **3** and **6** were introduced by superimposition of carbon atoms of the steroid skeleton with the corresponding atoms of 25*R*-Δ^7-DA, and maintaining the side chains in a fully extended conformation. Auspiciously, the MD analysis revealed that a clearly different binding mode was stabilized for each compound.

In the case of compound **3**, a ligand–receptor interaction similar to that observed previously for other *Ce*DAF-12 agonists was obtained. On one side, the 3-keto group forms a stable hydrogen bond with Gln^{638} during the whole length of the simulation (Figure 6A). At the other end of the steroid molecule, the terminal carboxy group participates in an extensive electrostatic network involving three arginine residues (Arg^{564}, Arg^{598} and Arg^{602}) and one aspartic acid residue (Asp^{532}). Regarding the steroid side chain, a fully extended conformation was favoured, with torsion angles C-20–C-22–C-23–C-24 (d_1), C-22–C-23–C-24–C-25 (d_2) and C-23–C-24–C-25–C-26 (d_3) fluctuating around 180° during the entire simulation. In order to investigate further the influence of the C-25 position on the dynamics behaviour of the steroid side chain, the ligand-binding mode of both Δ^4-DA epimers (25*S*–**1** and 25*R*–**1**) with a saturated side chain, was also analysed. MD trajectories of 20 ns of these systems revealed that, whereas in the 25*R* system, the favoured conformation of the side chain was also the fully extended one (d_1, d_2 and d_3 ~180°), the 25*S* isomer adopted a torsioned conformation (d_1 ~60°, d_2 ~180, d_3 ~60°) (Supplementary Figure S2). Similar findings have been reported for the (25*R*)-Δ^7-DA and (25*S*)-Δ^7-DA complexes using this model of *Ce*DAF-12 [19]. In this way, the MD analyses revealed that the reduction of the side-chain flexibility by the introduction of a double bond at C-24 does not impair the formation of a strong interaction between the carboxy group and the three arginine residues of the DAF-12 ligand-binding pocket, an interaction that is maintained with the steroid side chain in the fully extended conformation as in the 25*R* isomers.

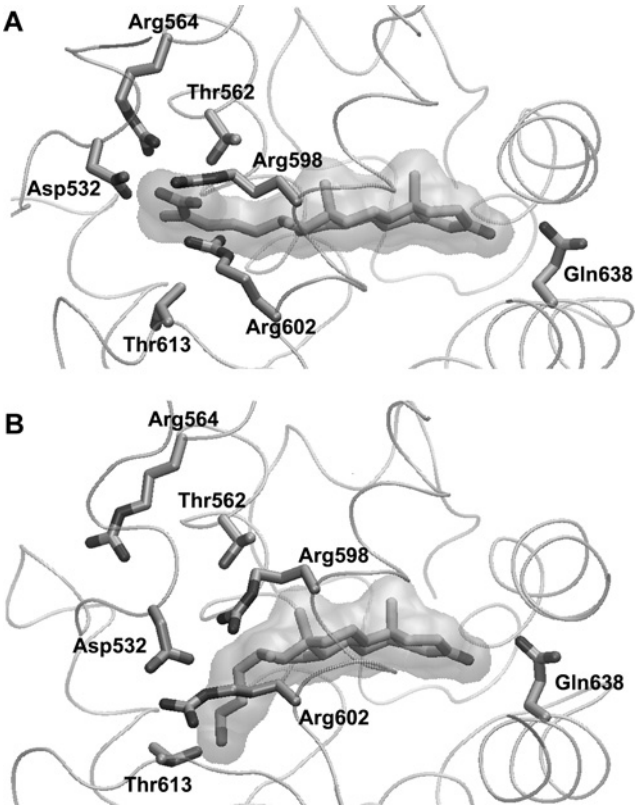

Figure 6 Ligand-binding mode of DA analogues

Representative snapshots of the *Ce*DAF-12–**3** (**A**) and *Ce*DAF-12–**6** (**B**) complexes during the MD simulation showing the polar interactions between the steroids and polar residues of the *Ce*DAF-12 ligand-binding pocket.

The analysis of compound **6** showed a dramatic change in its binding mode (Figure 6B). Similar to all agonist systems depicted above, the 3-keto group made a stable contact with Gln^{638}. However, at the other polar extreme of the molecule, the C-24 hydroxy did not interact with any of the arginine residues located in the receptor-binding pocket. Instead this hydroxy group formed a stable hydrogen bond with Thr^{613} that resulted in a major reorientation of the steroid side chain. This stabilized conformation was markedly different from that observed for compound **3**, with the side chain pointing towards the α face of the steroid. Since the interaction among arginine residues and the ligand is lost, these residues move away from each other, provoking an important rearrangement on the receptor structure. Notably, the stacking between guanidinium groups of Arg^{598} and Arg^{602}, observed in all agonist systems, disappears when compound **6** is bound. As this protein–protein interaction is often found in locations critical for receptor function [28], we propose that this conformational change would result in a non-functional DAF-12 conformation.

DISCUSSION

Steroid hormones promote their effects by binding to nuclear receptors which function as transcription factors that, in turn, regulate the expression of specific genes. Even small differences in ligand structures may result in dramatic changes in transcriptional activity and specificity of nuclear hormone receptors [29,30].

Access to a repertoire of different steroids with chemical modifications would enable the analysis of the relevance of these changes in nuclear receptor activity, opening the possibility of finding molecules that can regulate a specific set of genes and therefore might translate to important medicinal and agricultural uses.

DAF-12 shares similar structure with the vertebrate homologues VDR (vitamin D receptor), LXRs and FXR (farnesoid X receptor), which are targets of different cholesterol metabolites and are involved in essential functions, such as lipid regulation. In this context, finding how modifications performed on DA structures change the interaction with the DAF-12 receptor may contribute to shed light on the interaction of steroids with mammalian nuclear receptors. Having shown that the removal of the C-25 methyl group in Δ^4-DAs does not abolish DAF-12 activity [20], we continued to evaluate the effect of other modifications on the DA side chain. Compound **3** with a double bond at C-24 behaved as an agonist in reporter gene assays. Its activity (EC_{50} 0.8 μM) was comparable with the reported activity for (25*R*)-Δ^4-DA (EC_{50} >1 μM), but significantly less active than (25*S*)-Δ^4-DA (EC_{50} 0.1 μM) [9]. Since both compound **3** and (25*R*)-Δ^4-DA presented a ligand-binding mode in which a fully extended conformation of the steroid side chain is favoured, whereas the more active (25*S*)-Δ^4-DA exhibited a torsioned conformation, the activity of Δ^4-DAs may be correlated, at least in part, with the global conformation that the steroid side chain acquires in the ligand-binding pocket. Compound **3** also performed as a DAF-12 agonist *in vivo*, being able to rescue the *Daf-c* phenotype in *daf-9*(*dh6*) nematodes. It is known that *daf-9*(*dh6*) nematodes need different concentrations of exogenously added DAs to bypass dauer arrest and promote normal gonadogenesis and cuticle formation [12]. Thus the increase of DA levels would accelerate growth rate until it matches that of wild-type nematodes. Our results indicate that the amount of compound **3** bound to DAF-12 is high enough to bypass dauer diapause and promote adult programmes, but not to give a normal growth rate. Nevertheless, in both *in vitro* and *in vivo* assays, compound **3** showed more potent agonist DA activity than compound **2**.

Regarding analogues with shorter side chains, reporter gene assays showed that the C_{24} acid **4** retained some agonist activity on DAF-12. However, an increase of rigidity due to the introduction of a double bond at C-22 (compound **5**) or the replacement of the carboxy group by a hydroxy moiety (compound **6**) completely eliminated DAF-12 agonist activity. Notably, all C_{24} analogues were able to inhibit compound **3** action, with compounds **4** and **6** being stronger inhibitors than compound **5**. Taken together, these results obtained from reporter gene assays indicate that compound **4** acts as a partial agonist, whereas compound **6** behaves as a pure antagonist. Remarkably, wild-type *C. elegans* developed in the presence of compound **6** showed a slower development and a smaller size than untreated nematodes, indicating an *in vivo* antagonist effect. The delay in reaching progressive larval stages in the presence of this compound would suggest that programmes involved in developmental and reproductive control were not carried out properly, probably interfering with the action of DAF-12 target genes.

The experimental data obtained in the present study demonstrate that the polar group attached at the terminal carbon of the shortened steroid side chain modulates the global DAF-12 response. The analysis of the ligand-binding mode by molecular modelling suggested, as expected, that the C-24 hydroxy group does not interact with the positively charged arginine residues involved in the recognition of the negatively charged carboxy group of DAs. At variance with the carboxy group function, the uncharged hydroxy group can act as a hydrogen bond donor. In fact, according to the MD results, this hydroxy group would form a stable hydrogen bond with Thr^{613}, leading to a significant rearrangement on the receptor structure. Thus *Ce*DAF-12 would be able to recognize and bind compound **6**, but the resultant complex would not be able to induce gene transcription.

Since *C. elegans* and parasitic nematodes share the DA system as an endocrine core component for dauer and infective larvae formation, the studies related to *Ce*DAF-12 activity may provide a general strategy for controlling nematode parasitism in animals and plants.

AUTHOR CONTRIBUTION

Adalí Pecci, Olga Castro and Gerardo Burton conceived and designed the experiments. Gisela Samaja and Adriana Veleiro performed the chemistry. María Dansey performed *in vitro* experiments. Daiana Escudero and Olga Castro performed *in vivo* experiments. Lautaro Alvarez performed computational studies. María Dansey, Lautaro Alvarez, Adriana Veleiro, Adalí Pecci, Olga Castro and Gerardo Burton analysed the data and wrote the paper.

ACKNOWLEDGEMENTS

We thank Dr Adam Antebi (Max Planck Institute for Biology of Ageing, Cologne, Germany) for kindly providing *daf-9*(*dh6*) *dhEx24* strain and the *Caenorhabditis* Genetics Center for the *daf-9*(*rh50*) strain. We also thank Dr Daniel Hochbaum (Department of Medicine, University of Pittsburgh, Pittsburgh, PA, U.S.A.) for the plasmid pCMV myc DAF-12 A1, Dr Omar Coso (IFIBYNE-CONICET and Facultad de Ciencias Exactas y Naturales, Universidad de Buenos Aires, Buenos Aires, Argentina) for the pGL2 luciferase reporter construct containing the Gal4 upstream activating sequence (UAS) and Dr David Mangelsdorf (Howard Hughes Medical Institute and Department of Pharmacology, University of Texas Southwestern Medical Center at Dallas, Dallas, TX, U.S.A.) for the pCMX-Gal4-DAF-12LBD vector.

FUNDING

This work was supported by the Agencia Nacional de Promoción Científica y Tecnológica [grant numbers PICT 2010-0623 and PICT 2008-0700], Consejo Nacional de Investigaciones Científicas y Técnicas (CONICET) Argentina [grant numbers PIP 11220110100702 and PIP 11420080100567CO] and Universidad de Buenos Aires [grant number 20020100100281].

REFERENCES

1 Kenyon, C. (2010) A pathway that links reproductive status to lifespan in *Caenorhabditis elegans*. Ann. N.Y. Acad. Sci. **1204**, 156–162 CrossRef PubMed
2 Kaletta, T. and Hengartner, M. O. (2006) Finding function in novel targets: *C. elegans* as a model organism. Nat. Rev. Drug Discov. **5**, 387–398 CrossRef PubMed
3 Lapierre, L. R. and Hansen, M. (2012) Lessons from *C. elegans*: signaling pathways for longevity. Trends Endocrinol. Metab. **23**, 637–644 CrossRef PubMed
4 Butcher, R. A., Fujita, M., Schroeder, F. C. and Clardy, J. (2007) Small-molecule pheromones that control dauer development in *Caenorhabditis elegans*. Nat. Chem. Biol. **3**, 420–422 CrossRef PubMed
5 Golden, J. W. and Riddle, D. L. (1984) The *Caenorhabditis elegans* dauer larva: developmental effects of pheromone, food, and temperature. Dev. Biol. **102**, 368–378 CrossRef PubMed
6 Cassada, R. C. and Russell, R. L. (1975) The dauerlarva, a post-embryonic developmental variant of the nematode *Caenorhabditis elegans*. Dev. Biol. **46**, 326–342 CrossRef PubMed
7 Fielenbach, N. and Antebi, A. (2008) *C. elegans* dauer formation and the molecular basis of plasticity. Genes Dev. **22**, 2149–2165 CrossRef PubMed
8 Antebi, A. (2013) Steroid regulation of *C. elegans* diapause, developmental timing, and longevity. Curr. Top. Dev. Biol. **105**, 181–212 CrossRef PubMed
9 Motola, D. L., Cummins, C. L., Rottiers, V., Sharma, K. K., Li, T., Li, Y., Suino-Powell, K., Xu, H. E., Auchus, R. J., Antebi, A. and Mangelsdorf, D. J. (2006) Identification of ligands for DAF-12 that govern dauer formation and reproduction in *C. elegans*. Cell **124**, 1209–1223 CrossRef PubMed

10 Mahanti, P., Bose, N., Bethke, A., Judkins, J. C., Wollam, J., Dumas, K. J., Zimmerman, A. M., Campbell, S. L., Hu, P. J., Antebi, A. and Schroeder, F. C. (2014) Comparative metabolomics reveals endogenous ligands of DAF-12, a nuclear hormone receptor, regulating *C. elegans* development and lifespan. Cell Metab. **19**, 73–83 CrossRef PubMed
11 Shen, Y., Wollam, J., Magner, D., Karalay, O. and Antebi, A. (2012) A steroid receptor-microRNA switch regulates life span in response to signals from the gonad. Science **338**, 1472–1476 CrossRef PubMed
12 Schaedel, O. N., Gerisch, B., Antebi, A. and Sternberg, P. W. (2012) Hormonal signal amplification mediates environmental conditions during development and controls an irreversible commitment to adulthood. PLoS Biol. **10**, e1001306 CrossRef PubMed
13 Hochbaum, D., Zhang, Y., Stuckenholz, C., Labhart, P., Alexiadis, V., Martin, R., Knolker, H. J. and Fisher, A. L. (2011) DAF-12 regulates a connected network of genes to ensure robust developmental decisions. PLoS Genet. **7**, e1002179 CrossRef PubMed
14 Ludewig, A. H., Kober-Eisermann, C., Weitzel, C., Bethke, A., Neubert, K., Gerisch, B., Hutter, H. and Antebi, A. (2004) A novel nuclear receptor/coregulator complex controls *C. elegans* lipid metabolism, larval development, and aging. Genes Dev. **18**, 2120–2133 CrossRef PubMed
15 Wollam, J., Magner, D. B., Magomedova, L., Rass, E., Shen, Y., Rottiers, V., Habermann, B., Cummins, C. L. and Antebi, A. (2012) A novel 3-hydroxysteroid dehydrogenase that regulates reproductive development and longevity. PLoS Biol. **10**, e1001305 CrossRef PubMed
16 Gerisch, B., Weitzel, C., Kober-Eisermann, C., Rottiers, V. and Antebi, A. (2001) A hormonal signaling pathway influencing *C. elegans* metabolism, reproductive development, and life span. Dev. Cell **1**, 841–851 CrossRef PubMed
17 Jia, K., Albert, P. S. and Riddle, D. L. (2002) DAF-9, a cytochrome P450 regulating *C. elegans* larval development and adult longevity. Development **129**, 221–231 PubMed
18 Martin, R., Entchev, E. V., Kurzchalia, T. V. and Knolker, H. J. (2010) Steroid hormones controlling the life cycle of the nematode *Caenorhabditis elegans*: stereoselective synthesis and biology. Org. Biomol. Chem. **8**, 739–750 CrossRef PubMed
19 Alvarez, L. D., Arroyo Manez, P., Estrin, D. A. and Burton, G. (2012) The *Caenorhabditis elegans* DAF-12 nuclear receptor: structure, dynamics, and interaction with ligands. Proteins **80**, 1798–1809 PubMed
20 Samaja, G. A., Castro, O., Alvarez, L. D., Dansey, M. V., Escudero, D. S., Veleiro, A. S., Pecci, A. and Burton, G. (2013) 27-Nor-Δ^4-dafachronic acid is a synthetic ligand of *Caenorhabditis elegans* DAF-12 receptor. Bioorg. Med. Chem. Lett. **23**, 2893–2896 CrossRef PubMed
21 Gioiello, A., Sabbatini, P., Rosatelli, E., Macchiarulo, A. and Pellicciani, R. (2011) Divergent and stereoselective synthesis of dafachronic acids. Tetrahedron **67**, 1924–1929 CrossRef
22 Cheatham, III, T. E., Cieplak, P. and Kollman, P. A. (1999) A modified version of the Cornell et al. force field with improved sugar pucker phases and helical repeat. J. Biomol. Struct. Dyn. **16**, 845–862 CrossRef PubMed
23 Berendsen, H. J. C., Postma, J. P. M., Van Gunsteren, W. F., DiNola, A. and Haak, J. R. (1984) Molecular dynamics with coupling to an external bath. J. Chem. Phys. **81**, 3684–3690 CrossRef
24 Mooijaart, S. P., Kuningas, M., Westendorp, R. G., Houwing-Duistermaat, J. J., Slagboom, P. E., Rensen, P. C. and van Heemst, D. (2007) Liver X receptor α associates with human life span. J. Gerontol. A Biol. Sci. Med. Sci. **62**, 343–349 CrossRef PubMed
25 Gerisch, B., Rottiers, V., Li, D., Motola, D. L., Cummins, C. L., Lehrach, H., Mangelsdorf, D. J. and Antebi, A. (2007) A bile acid-like steroid modulates *Caenorhabditis elegans* lifespan through nuclear receptor signaling. Proc. Natl. Acad. Sci. U.S.A. **104**, 5014–5019 CrossRef PubMed
26 Albert, P. S. and Riddle, D. L. (1983) Developmental alterations in sensory neuroanatomy of the *Caenorhabditis elegans* dauer larva. J. Comp. Neurol. **219**, 461–481 CrossRef PubMed
27 Gerisch, B. and Antebi, A. (2004) Hormonal signals produced by DAF-9/cytochrome P450 regulate *C. elegans* dauer diapause in response to environmental cues. Development **131**, 1765–1776 CrossRef PubMed
28 Flocco, M. M. and Mowbray, S. L. (1994) Planar stacking interactions of arginine and aromatic side-chains in proteins. J. Mol. Biol. **235**, 709–717 CrossRef PubMed
29 Brown, A. J. and Slatopolsky, E. (2008) Vitamin D analogs: therapeutic applications and mechanisms for selectivity. Mol. Aspects Med. **29**, 433–452 CrossRef PubMed
30 Singarapu, K. K., Zhu, J., Tonelli, M., Rao, H., Assadi-Porter, F. M., Westler, W. M., DeLuca, H. F. and Markley, J. L. (2011) Ligand-specific structural changes in the vitamin D receptor in solution. Biochemistry **50**, 11025–11033 CrossRef PubMed

Received 3 July 2014/27 August 2014; accepted 6 November 2014
Published as BJ Immediate Publication 6 November 2014, doi:10.1042/BJ20140833